Atmos. Meas. Tech. Discuss., https://doi.org/10.5194/amt-2018-160
Manuscript under review for journal Atmos. Meas. Tech.
Discussion started: 3 July 2018

Atmospheric Measurement Techniques Discussions

Metrology of the Solar Spectral Irradiance at the Top Of Atmosphere in the Near Infrared Measured at Mauna Loa Observatory: The PYR-ILIOS campaign

Nuno Pereira[1], David Bolsée[1], Peter Sperfeld[2], Sven Pape[2], Dominique Sluse[1], and Gaël Cessateur[1]

[1]BIRA-IASB, 3 Ringlaan, 1180 Brussels, Belgium
[2]Physikalisch-Technische Bundesanstalt, Braunschweig, Germany

Correspondence to: nuno.pereira@aeronomie.be

Abstract. The near infrared (NIR) part of the solar spectrum is of prime importance for the solar physics and climatology, directly intervening in the Earth's radiation budget. Despite its major role, available solar spectral irradiance (SSI) NIR datasets, space-borne or ground based, present discrepancies caused by instrumental or methodological reasons. We present new results obtained from the PYR-ILIOS campaign, which is a replication of the previous IRSPERAD campaign which took place in 2011 at the Izaña Observatory (IZO). We used the same instrument and primary calibration source of spectral irradiance. A new site was chosen for PYR-ILIOS: the Mauna-Loa observatory in Hawaii (3397 m asl), approximately 1000 m higher than IZO. Relatively to IRSPERAD, the methodology of monitoring the traceability to the primary calibration source was improved. The results as well as a detailed error budget are presented. We demonstrate that the most recent results, from PYR-ILIOS and other space-borne and ground-based experiments show an NIR SSI lower than ATLAS3 for wavelengths above $1.6\mu m$.

1 Introduction

An accurate knowledge of the solar spectral irradiance (SSI) remains central to the study of the climate on Earth. The variability in the ultraviolet (UV) part of the spectrum and its influence on climate via the mechanisms of solar-terrestrial interactions, simulated by chemistry-climate models (CCM) (Gray et al. (2010), Ermolli et al. (2013)), make up for the most of the research in SSI measurements. Despite of its extremely low variability ($< 0.05\%$ over a solar cycle (Lean (1991),Harder et al. (2009)), the near-infrared (NIR) part of the spectrum plays a major role in the Earth's radiative budget due to its quasi-total absorption by water vapour (**?**). The determination of its absolute level remains challenging. The measurement of the top of atmosphere (TOA) SSI started nearly 50 years ago and evoluted both with ground-based and space borne instruments, a consensus on the absolute level in the NIR part is still to be achieved.

Aircraft borne instrumentation at an altitude of 12 km provided the first TOA SSI measurements dataset in 1969 (Arvesen et al. (1969)) with an onboard standard of spectral irradiance. Several ground-based measurements campaigns in the UV, Visible and NIR, have been conducted from the top two mountain-top reference sites:

- Izaña Atmospheric Observatory (IZO): IRSPERAD (Bolsée et al. (2014)) with a NIR (0.6 μm - 2.3μm) spectroradiometer and the QASUMEFTS (Gröbner et al. (2017)) instrument providing a High-resolution UV spectrum; both were

Atmos. Meas. Tech. Discuss., https://doi.org/10.5194/amt-2018-160
Manuscript under review for journal Atmos. Meas. Tech.
Discussion started: 3 July 2018

Atmospheric Measurement Techniques Discussions

calibrated against the Physikalisch-Technische Bundesanstalt (PTB) BB3200gb blackbody (Sapritsky et al. (1997),Sperfeld et al. (1998a, 2000));

– Mauna Loa Observatory (MLO): Shaw (1982) with a 10-channel (UV, Visible and NIR) filter radiometer; Gröbner and Kerr (2001) with a double Brewer spectrophotometer measuring in the 300 nm - 355nm; Kindel et al. (2001) provided TOA SSI in the range 350 nm to 2500 nm, measured with a spectroradiometer; all these measurement campaigns used different types of 1000W lamps, traceable to National Institute of Standards and Technology (NIST) standards as calibration sources.

Finally, the CAVIAR (Menang et al. (2013)) and CAVIAR2 (Elsey et al. (2017)) spectra, obtained with an infrared Fourier spectrometer (FTIR) calibrated against National Physical Laboratory (NPL) standards at the United Kingdom Met Observation site in Carbone, in the range 1 μm - 2.5μm.

TOA SSI values from all referred ground-based campaigns were obtained with the Langley-plot technique that permits the extrapolation to the TOA irradiance in criteriously chosen atmospheric windows (Section 2.2). The monitoring of the absolute spectral calibrations is secured by comparisons with relative stable secondary standards. The traceability to primary irradiance standards is, therefore, an advantage for ground based measurement. Performing these measurements based on world reference sites for the determination of TOA physical quantities, such as IZO and MLO, on often occurring pristine day conditions ensures a high accuracy of the TOA extrapolations (Shaw (1975, 1976),Kiedron and Michalsky (2016)).

On the other hand, space borne SSI measurements covering the NIR range, started in the 1990s, however limited to wavelengths shorter than 2.4 μm. The SOLSPEC (SOLar SPECtrum) instrument on board EURECA (Thuillier et al. (1981)) that pionereed the space-borne NIR absolute solar spectroscopy released the ATLAS3 reference spectrum (Thuillier et al. (2003)). An upgraded version (SOLAR/SOLSPEC), including a fully refurbished NIR channel, readout electronics and extended wavelength range up to 3.2 μm of SOLSPEC flew from 2008-2017 on board the International Space Station (ISS) (Thuillier et al. (2009)), releasing the SOLAR 2 (Thuillier et al. (2013)), SOLAR/SOLSPEC (Bolsée (2012)) and SOLAR-ISS(IR) (Meftah et al. (2017)); it is nowadays the instrument that measured farther the SSI in the NIR. The instrument providing the longest time series of SSI measurements in the NIR is the SIM (Spectral Irradiance Monitor) prism spectrometer on SORCE (Solar Radiation and Climate Experiment) launched in 2003 (Harder et al. (2000a),Harder et al. (2005)) and still on orbit but with scarce operational time, due to the end of battery life. Another instrument contributing to NIR SSI measurements is SCIAMACHY (Scanning Imaging Absorption Spectrometer for Atmospheric Cartography) (Noël et al. (1998)), a remote sensing spectrometer adapted to measure SSI. The latest data release is SCIAMACHY V9 (Hilbig et al. (2018)).

All above referred NIR datasets reasonably agree till 1.3μm. SORCE due to its incompatibility with the Total Solar Irradiance (TSI) (Harder et al. (2010)) has been scaled up to ATLAS3 in the NIR and, consequently, differences between both don't exceed 2% in the NIR range. At 1.6μm, corresponding to the minimum opacity value of the solar photosphere, differences up to 8% (reaching 10% at 2.2μm) are observed between ATLAS3 with respect to SOLAR/SOLSPEC.

Atmos. Meas. Tech. Discuss., https://doi.org/10.5194/amt-2018-160
Manuscript under review for journal Atmos. Meas. Tech.
Discussion started: 3 July 2018

Atmospheric Measurement Techniques Discussions

This difference motivated the development of new ground-based instrumentation measuring the SSI NIR: CAVIAR and IRSPERAD. The data of both experiments confirmed this bias while at the same time SOLSPEC and SCIAMACHY data reprocessing tend to intermediate values between ATLAS3 and SOLAR/SOLSPEC.

In this paper we present a re-run of the IRSPERAD experiment, named PYR-ILIOS, carried out in July 2016. While still using the Langley plot technique and calibration against the PTB blackbody, this new experiment differs from IRSPERAD in three aspects: first, the observation site is MLO instead of IZO, second, possible sources of systematic uncertainties have been identified and fixed (see Sec. 2.1), third, the traceability of the calibration to the primary standard was improved (see Sec. 2.5). A detailed estimation of the uncertainty budget will be presented in Sec. 3, followed by the presentation of the obtained spectrum and its comparison with space borne and ground-based spectra described in this chapter along with a discussion on the status of the NIR SSI measurement.

2 Methods

2.1 Instrumentation

The core of the direct Sun measurement instrumentation is a Bentham NIR spectrometer: it consists of double monochromator placed inside a thermally stabilized container, with light detection by a PbS cell. A fiber optic guides the Sun light between the entry slit of the spectrometer and a 7.2° field-of-view (FOV) Sun light-collecting optics (telescope). The telescope is connected to an EKO Sun tracker that provides a tracking accuracy of $\pm 0.1^\circ$. The working wavelength range is from 0.6 μm to 2.3 μm, with a nominal 10 nm bandpass. The instrument characteristics are given in depth in Bolsée et al. (2014) and have remained unchanged since. No modifications have been made neither to the telescope nor to the spectrometer. Nevertheless, a failure in the assemblage of the components was detected and rectified: the lens focusing the light collected in the optic fiber into the detector entry slit was properly fixed into its barrel support for the PYR-ILIOS campaign, which wasn't previously the case for the IRSPERAD campaign. The lens was most likely loose during the measurement campaign described in Bolsée et al. (2014), at IZO. Another change relative to the IRSPERAD campaign was that the thermally stabilized spectrometer container was placed indoors in a thermally stabilized environment, which reduced thermal stress due to outdoor exposure and improved the stability of the spectrometer's response.

2.2 Langley-plot method

The wavelength-dependent direct transmitted solar irradiance in the atmosphere is described by the Beer-Bouguer-Lambert law:

$$I(\lambda) = I_0(\lambda) D^{-2} \exp\left[-m(\theta)\tau(\lambda)\right], \quad (1)$$

where I is the irradiance at the top of atmosphere (TOA), m is the air mass factor (AMF) as a function of the solar zenith angle (SZA) θ, and τ is the optical depth that depends on λ. D, is the Earth-Sun distance at the moment of the measurement. Taking

Atmos. Meas. Tech. Discuss., https://doi.org/10.5194/amt-2018-160
Manuscript under review for journal Atmos. Meas. Tech.
Discussion started: 3 July 2018

Atmospheric Measurement Techniques Discussions

the logarithm, Eq. 1 it can be re-written:

$$\log\left[I\left(\lambda\right)\right] = \log\left[I_0\left(\lambda\right) D^{-2}\right] - m\left(\theta\right)\tau\left(\lambda\right). \tag{2}$$

Provided that atmospheric absorption is negligible and $\tau\left(\lambda\right)$ remains constant for a series of measurements of $I_0\left(\lambda\right)$ taken over a given range of $m\left(\theta\right)$ (generally spreading over a half day), the TOA value of $I_0\left(\lambda\right)$ is thus the intercept at the origin ($m = 0$) of the least squares regression to the data series $I\left(\lambda\right)$ as a function of m. Equation 2 is only applicable to atmospheric regions where the contributions to optical depth are limited to aerosol and Rayleigh scattering. It is thus not valid in spectral bands of absorption due to atmospheric constituents, namely CO_2, O_2, O_3 and H_2O without a modification as described by Schmid and Wehrli (1995).

2.3 Atmospheric windows

The wavelength domains for which the Langley-plot method described in 2.2 is valid, atmospheric windows, were determined by model on a procedure developed in Kindel et al. (2001) and also used in Bolsée et al. (2014): using a TOA reference spectrum as input, MODTRAN was used to simulate irradiances measured at ground, giving the measurement site parameters, for a series of AMFs. The Langley-plot method was applied to these simulated irradiances and the wavelengths for which the synthetic I_0 recreated the input TOA within 0.5% were kept as valuable wavelengths for the Langley-plot; these set of wavelengths were grouped in contiguous windows called atmospheric windows.

2.4 Absolute Calibration

The absolute calibration was performed against a primary standard of spectral irradiance, the BB3200pg blackbody of the PTB. It has been extensively described in Sapritsky et al. (1997) and Sperfeld et al. (1998a, 2000). The spectral irradiance equation describing the black body emission is calculated using Planck's law:

$$E_{\mathrm{BB}}(\lambda) = \varepsilon_{\mathrm{BB}} \frac{A_{\mathrm{BB}}}{d_{\mathrm{BB}}^2} \frac{c_1}{n^2.\lambda^5} \frac{1}{\exp\left(\frac{c_2}{n_\lambda.\lambda.T_{\mathrm{BB}}}\right) - 1} \tag{3}$$

Where $\varepsilon_{\mathrm{BB}}$ and A_{BB} stand, respectively, for the effective emissivity and the aperture of the BB3200pg, d_{BB} for the distance between the blackbody aperture and the optic center of the entrance optics, n for the refractive index of air, c_1 and c_2 are the first and second radiation constants.

The fundamental parameter, the temperature of the cavity T is known with a standard uncertainty of 0.5 K ($\sim 0.02\%$ for a nominal temperature of 3000K) with a drift lower than $0.5\ \mathrm{Kh}^{-}1$ (Friedrich et al. (1995),Werner et al. (2000),Taubert et al. (2003)). The uncertainties on $\varepsilon_{\mathrm{BB}}$, A_{BB} and d_{BB} are 0.01%, 0.04% and 0.004%, respectively.

The absolute calibration coefficient R, that converts the spectrometer signal into irradiance is given by Eq. 4:

$$R(\lambda) = \frac{E_{\mathrm{BB}}(\lambda, T)}{S_{\mathrm{BB}}(\lambda)} \tag{4}$$

Atmos. Meas. Tech. Discuss., https://doi.org/10.5194/amt-2018-160
Manuscript under review for journal Atmos. Meas. Tech.
Discussion started: 3 July 2018

With S_{BB} being the signal recorded by the spectrometer and E_{BB}, the emission of the blackbody, given by Eq. 3. During the calibration campaign at PTB, two different temperatures set points, 3016.5K and 2847.6K, were used to build the response curve, R_{BB}, and to verify the linearity of the spectrometer. The distance d_{BB} was kept fixed at 1384.05 mm so that the blackbody aperture was seen by the entrance optics with an angular extension of $0.5°$.

2.5 Relative Calibration

A set of 6 FEL lamps (F102, F104, F417, F418, F545, F546) were used as relative calibration standards, to monitor a possible change of response of the spectrometer during the measurement campaign. Taking as reference the lamps signal measured at the PTB (April 27), $S_{Fj}^{PTB}(\lambda)$, four additional relative calibrations were performed:

- Immediately before the start of the measurement campaign on June 29, the signal of the 6 lamps, S_{Fj}^{MLO1}, was measured on site. This first MLO relative calibration was valuable to monitor the spectrometers response change between the calibration at PTB and the beginning of the field measurements. During this 2-month period that included the transportation of the equipment, a decrease of response varying between 1% and 3% in the 1000 nm to 2200 nm range was detected.

- During the 20-day measurement campaign three relative calibrations were performed: on July 7, 14 and 19. The cumulated loss of response between June 29 and July varied from 1.5% to 0.5% in the $800nm$ to $1.8\mu m$ domain.

The corresponding correction factor for each relative calibration is:

$$K_i(\lambda) = \frac{1}{N}\sum_{j}^{N}\frac{S_j^{MLOi}(\lambda)}{S_j^{PTB}(\lambda)} \tag{5}$$

Where N stands for the total number of lamps and j to the lamp number. $K_i(\lambda)$ was obtained by linear interpolation for all days of the campaign.

2.6 Ground-based campaign

The PYR-ILIOS campaign took place during the first 20 days of July 2016 at the Mauna Loa Observatory (MLO) in the island of Hawaii. MLO (19.53° N,155.58°W) is situated at 3397 m above sea level; it is the leading long-term atmospheric monitoring facility on earth, a primary calibration site for the AERONET network, a global station for the Global Atmosphere Watch (GAW) of the World Meteorological Organization (WMO) and the premier site[1] for the measurement of the concentration of atmospheric carbon dioxide. MLO is a direct-Sun calibration site of the AErosol Robotic NETwork (AERONET[2]). It is considered a world reference site to accurately determine extraterrestrial constants via the Langley-plot method (Shaw (1975, 1976),Kiedron and Michalsky (2016)).

[1]https://www.esrl.noaa.gov/gmd/obop/mlo/programs/esrl/co2/co2.html
[2]https://aeronet.gsfc.nasa.gov/

Atmos. Meas. Tech. Discuss., https://doi.org/10.5194/amt-2018-160
Manuscript under review for journal Atmos. Meas. Tech.
Discussion started: 3 July 2018

Atmospheric Measurement Techniques Discussions

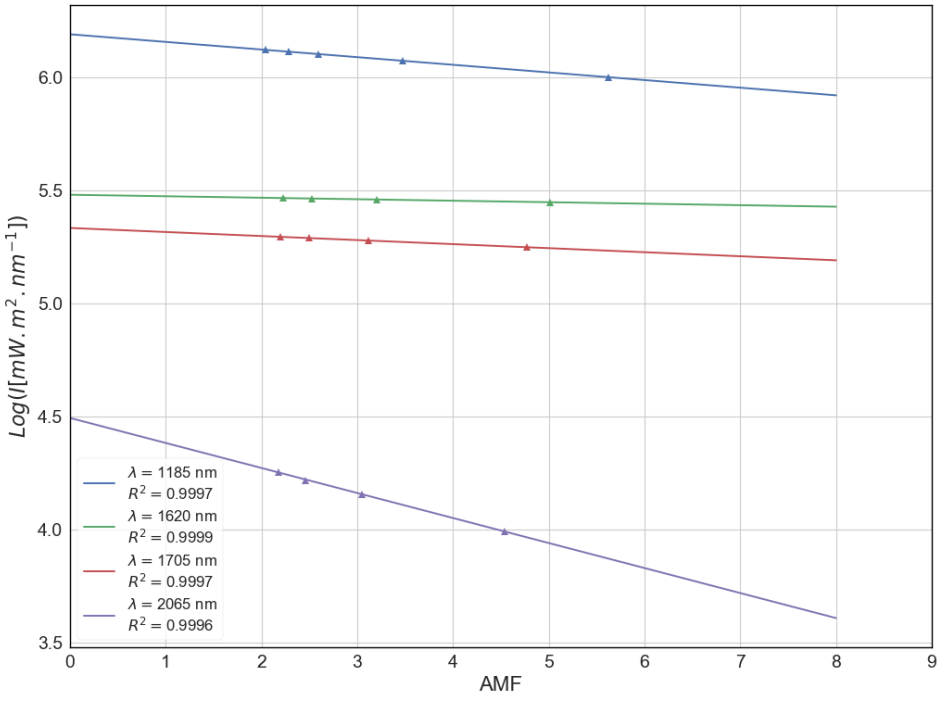

Figure 1. Langley plot for the morning of the July 2, for selected high quality Langley-plots.

2.7 Data selection and analysis

Spectra measured at AMF between 2 and 8 are used for the Langley-plot method. AMF are calculated using the Kasten and Young algorithm (Kasten and Young (1989)). Solar Zenithal Angles (SZA) are calculated with NOAA Solar Position Calculators[3] algorithm, based on Meeus (1998).

From the 20-day campaign, 8 high-quality half-days, all during morning time, were kept for analysis. The selection criteria were: verification of cloudless clear skies, a Langley-plot correlation coefficient $R^2 > 0.9$ and aerosol optical depth (AOD) variation no higher than 10% during the period of the measurement. This last criterion was verified using data from the the AERONET network, simultaneously for the wavelengths of 870 nm, 1020 nm and 1640 nm. The day's list and respective AOD variation criteria can be consulted in A1. An example of Langley plot is shown in Fig. 1.

Atmos. Meas. Tech. Discuss., https://doi.org/10.5194/amt-2018-160
Manuscript under review for journal Atmos. Meas. Tech.
Discussion started: 3 July 2018

Atmospheric Measurement Techniques Discussions

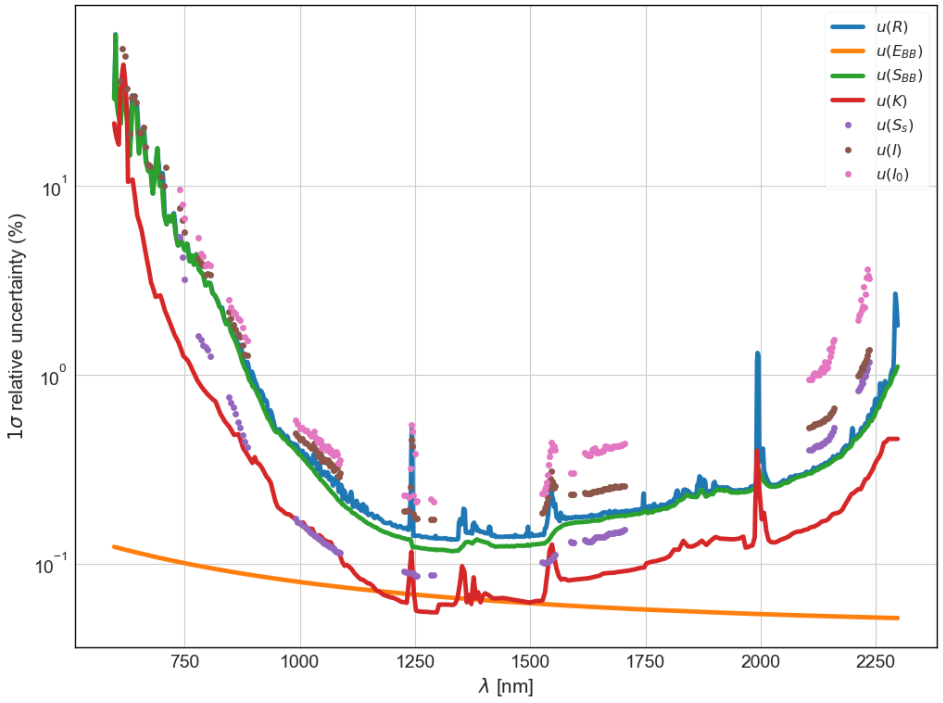

Figure 2. Individual uncertainties contributing to the uncertainty in the TOA SSI, $u(I_0)$. Blackbody ($u(E_{BB})$, $u(S_{BB})$ and $u(R)$) and Lamps ($u(K)$) associated quantities are plotted for the full wavelength working range, while solar measurement associated quantities ($u(S_s)$, $u(I)$ and $u(I_0)$) are plotted in the atmospheric windows wavelengths.

3 Uncertainty budget

3.1 Uncertainty on the spectrometer signal

The raw uncertainty of a spectrometer measured signal, S_x^{raw} regardless of its source, either Solar (S_S), blackbody (S_{BB}) or lamps $\left(S_{Fj}^{PTB}, S_{Fj}^{MLO}\right)$ signal, is a function of the intrinsic noise of the measurand physical signal convolved by the spectrometer's total transmission and detector's response. The uncertainty on a measured signal is expressed by the Signal-to-Noise Ratio (SNR) curve. The SNR curve, shown in Fig. A1, was determined in laboratory by calculating the ratio between the mean and standard deviation for a series of different intensity signals of a 1000W stable lamp (Bolsée et al. (2014)). Additionally, all measured signals, $S_x^{raw}(\lambda)$, are affected by an uncertainty term due to the finite bandpass of the instrument ($u(C_{\Delta\lambda})$), and the

[3]https://www.esrl.noaa.gov/gmd/grad/solcalc/index.html

Atmos. Meas. Tech. Discuss., https://doi.org/10.5194/amt-2018-160
Manuscript under review for journal Atmos. Meas. Tech.
Discussion started: 3 July 2018

Atmospheric Measurement Techniques Discussions

uncertainty on the determination of the true wavelength scale ($u(C_\lambda)$).

$$u(S_x(\lambda))^2 = u(S_x^{raw}(\lambda))^2 + u\left[C_\lambda(S_x^{raw}(\lambda), \delta(\lambda))\right]^2 + u\left[C_{\Delta\lambda}(S_x^{raw}(\lambda), BW)\right]^2 \quad (6)$$

Where $\delta(\lambda)$ stands for the maximum deviation in the determination of the real wavelength scale of the spectrometer. $\delta(\lambda)$ was determined in laboratory by measuring the deviation between the central wavelength of and its corresponding nominal value of a series of well known emission peaks of Xe, Ar and Ke lamps as well as of lasers and pen-ray lamps; $\delta(\lambda) < 0.2nm$ for the working wavelength range. BW stands for the spectrometer bandpass, 10.63 nm measured in laboratory.

3.2 Uncertainty on a calibrated direct Sun measurement

The expression for a calibrated solar measurement, $I(\lambda)$ is:

$$I(\lambda) = S_S(\lambda).R(\lambda).K(\lambda), \quad (7)$$

With $S_S(\lambda)$, $R(\lambda)$ and $K(\lambda)$ being expressed by Eq. 6, 4 and 5, respectively. The uncertainty on $I(\lambda)$, $u(I(\lambda))$ is calculated by application of the Law of Propagation of Uncertainties (LPU) to Eq. 7; this uncertainty as well as the ones associated to the coefficients, $R(\lambda)$ and $K(\lambda)$, $u(R)$ and $u(K)$, are represented in Fig. 2. The similarity of shapes of the curves of the individual uncertainties reflects the convolution of the measured signals by the spectrometer's response. The largest contribution to the calibrated solar signal comes from the uncertainty on the absolute calibration which is dominated by the uncertainty $u(S_{BB})$ of measured signal S_{BB} of the blackbody irradiance, whereas the uncertainty on the emission of the blackbody, $u(E_{BB})$ is known within 0.1% for the quasi-totality of the wavelength range. The use of 6 FEL lamps permits the reduction of $u(K)$ of a factor ~ 2, comparatively to the use of 1 lamp.

3.3 Uncertainty on the determination of the TOA irradiance

The uncertainty in the determination of the TOA irradiance, $u(I_0)$ corresponds to the uncertainty on the determination of the intercept at origin, P_0, when applying a linear regression on Eq. 2. The uncertainty on the measured I in the Langley-plot method logarithmic space, $u(log(I))$ and the uncertainty in the $u(I_0)$ irradiance value are given by:

$$u^2(log(I)) = \left(\frac{\partial log(I)}{\partial I}\right)^2 .u^2(I) = \left(\frac{u(I)}{I}\right)^2 \quad (8)$$

$$u^2(I_0) = \left(\frac{\partial exp(P_0)}{\partial P_0}\right)^2 .u^2(P) = exp(P_0)^2 .u^2(P_0) \quad (9)$$

Where, $I_0 = exp(P_0)$ gives the irradiance TOA value. The uncertainty in P was estimated by 2 independent methods.

- A Monte Carlo method: given a measured langley plot dataset consisting of $(m_i, log(I_i))$ points, a new synthetic dataset $(m_i, log(I_i^*)))$ is created where each $log(I_i^*)$ is affected by a random normal distributed quantity, with a standard uncertainty given by Eq.8. The standard deviation in the distribution of the $N >> 1$ retrieved P_0, corresponds to $u(P_0)$, with $u(I_0)$ given by Eq. 9.

Atmos. Meas. Tech. Discuss., https://doi.org/10.5194/amt-2018-160
Manuscript under review for journal Atmos. Meas. Tech.
Discussion started: 3 July 2018

– The weighted total least-squares (WTLS) algorithm developed Krystek and Anton (2007) was used. It computes the uncertainty in the determination both linear regression parameters using the uncertainties on the measured quantities as inputs; the uncertainties on AMF are considered zero.

The uncertainty on the determination of the TOA irradiance, $u(I_0)$, matches perfectly for both methods; it is below 1% for the central wavelength range of $1.0\mu m$ to $2.0\mu m$. Figure 2 shows the contribution of all the uncertainty terms detailed in Sec. 3;

3.4 Quantification of the circumsolar radiation

An ideal sun-collecting optic device should ideally have an acceptance angle equal to that of the solar disk seen on earth, i.e. $\sim 0.5^\circ$. In practice the FOV of is much larger than 0.5° such that the Sun sky-scattered radiation enters the FOV of the sun-collecting optics, affecting the direct normal Sun measurement. Circumsolar radiation is strongly dependent on aerosols size and its abundance, increasing with AMF and decreasing with wavelength due to Rayleigh scattering, (Blanc et al. (2014)). The estimation of circumsolar radiation was done with the aid of the LibRadtran (Mayer and Kylling (2005)) radiative transfer model (RTM). LibRadtran computes the radiance field of the sun sky-scattered radiation. The integral of this radiance field over the solid angle of the acceptance cone of the entrance optics is the amount of circumsolar irradiance (CSI) measured by the spectrometer in excess of the normal direct Sun irradiance (DNI) (Gueymard (2001)). For standard clear-sky atmospheric conditions observed at MLO, for aerosol charges values as the ones shown, the quantification of CSI is shown in Fig. A2. Given the uncertainty budget, the impact of the circumsolar radiation can be considered negligible.

4 Results

The PYR-ILIOS TOA SSI results are obtained by averaging the $I_\lambda(0)$ obtained by the Langley-plot method for the 8 half-days that satisfied the data selection criteria detailed in Section 2.7. They are compared to the space-borne and ground-based instruments described in the Introduction. SOLAR-ISS(IR) from Meftah et al. (2017) is choosen as the reference spectrum for the comparison. The mismatch between the PYR-ILIOS and IRSPERAD dataset, varies between 2% and 4% in the central wavelength range between $1.0\mu m$ to $1.8\mu m$, attaining 5% in the $2.1\mu m$ window and peaking to a maximum of 6% in the $1.5\mu m$ and $2.2\mu m$ windows. Except for the shorter wavelengths ($\lambda < 900nm$) region, error bars don't explain the observed mismatch between both. PYR-ILIOS is in excellent agreement with SCIAMACHY V9, Kindel and SOLAR-ISS(IR) in the $1.6\mu m$ region. For wavelengths above $2\mu m$ PYR-ILIOS and Kindel are in excellent agreement; the level of the two SCIAMACHY V9 adjacent bands ($1.9\mu m - 2.05\mu m$ and $2.2\mu m - 2.4\mu m$) suggests that also SCIAMACHY V9 is in agreement with both. The higher disagreement is observed in the far end of the spectrum, with discrepancies of up to 13% between CAVIAR2 and ATLAS3 and SORCE. Below $1.3\mu m$ the disagreement between datasets is minimal

Atmos. Meas. Tech. Discuss., https://doi.org/10.5194/amt-2018-160
Manuscript under review for journal Atmos. Meas. Tech.
Discussion started: 3 July 2018

Atmospheric Measurement Techniques Discussions

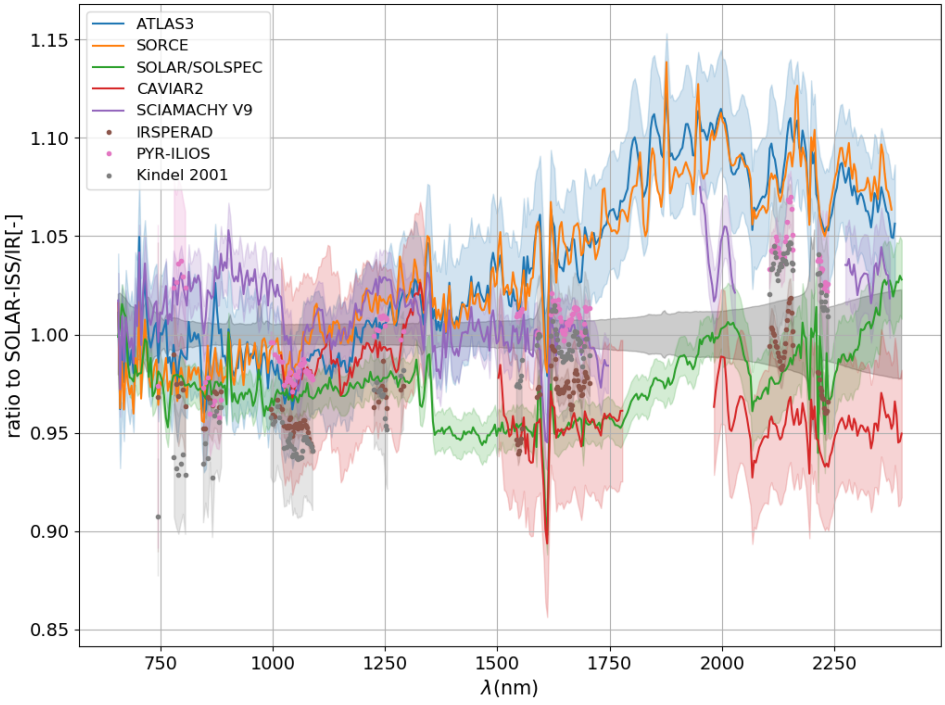

Figure 3. Ratio of ground-based and space-borne spectra and respective error bars at $\pm 1\sigma$, relative to SOLSPEC-ISS(IR)

5 Discussion

The difference observed between IRSPERAD and PYR-ILIOS is not explained by the error bars of both datasets. An atmospheric bias is not considered, because MLO and IZO are world reference sites for the determination of extra-terrestrial constants (Shaw (1976), Kiedron and Michalsky (2016)) and the atmospheric perturbation in ground-based SSI measurements are negligible (Elsey et al. (2017), Bolsée et al. (2016), Weber (2015)). By carrying the new PYR-ILIOS experiment, we unveiled a defect of fixation of the focusing lens. Due to the fact that the instrument was moved between the IRSPERAD pre-campaign relative calibration (May 31 2011) and the start of the Sun measurement campaign (June 1 2011 onwards), the effect of the lens' eventual movement was impossible to be monitored; this defect likely biased the SSI obtained during the IRSPERAD campaign. This defect was detected and corrected for the PYR-ILIOS campaign and the relative calibration strategy adapted to identify possible similar issues: the instrument was installed, powered on and the lamps were measured; the solar measurements began immediately afterwards, without displacing nor powering off the instrument. The PYR-ILIOS relative calibration procedure highlights the importance of ground-based pre-campaign instrument's response monitoring with secondary stan-

dards. Additionally it justifies the choice of PYR-ILIOS as the more reliable measurement due to the high confidence of the traceability of the instrument's calibration to the blackbody primary standard.

The NIR SSI absolute level debate although not concluded, has been significantly enriched with the data reanalysis of space instruments as for SOLSPEC/SOLAR and SCIAMACHY and the rerun of ground-based campaigns as it is the case for the presented PYR-ILIOS campaign. Relative to the $\sim 8\%$ difference observed between first SOLSPEC/SOLAR data product, SOLAR/SOLSPEC, and ATLAS3 and SORCE, an intermediate level between both shown by SCIAMACHY V9, SOLSPEC-ISS(IR), PYR-ILIOS and Kindel 2001, suggests a convergence in this wavelength range. For wavelengths above $2\mu m$, SOLSPEC-ISS(IR) is compatible with its predecessor SOLAR/SOLSPEC, while SCIAMACHY V9, Kindel 2001 and PYR-ILIOS, are closer to ATLAS3 and SORCE.

Data from SORCE sucessor, TSIS on board ISS since December 2017, is expected to further increase the understanding of the SSI in the NIR.

Data availability. The PYR-ILIOS NIR SSI dataset can be downloaded at ftp://ftp-ae.oma.be/dist/PYRILIOS_NIR_SSI/

Acknowledgements. The authors which to thank the staff of the Mauna Loa Observatory for kindly supporting the campaign and especially Paul Fukumura-Sawada of the NOAA Earth System Research Laboratory. We thank Brent Holben, PI of MLO AERONET site, for his efforts in establishing and maintaining the MLO site. The authors acknowledge the support from the Belgian Federal Science Policy Office (BELSPO) through the ESA-PRODEX program (contract 4000110593 extension of PEA for 2016-2017) and the funding of the Solar-Terrestrial Centre of Excellence (STCE).

References

Arvesen, J. C., Griffin, R. N., and Pearson, D. J.: Determination of extraterrestrial solar spectral irradiance from a research aircraft, Appl. Opt., 8, 2215–2232, 1969.

Blanc, P., Espinar, B., Geuder, N., Gueymard, C., Meyer, R., Pitz-Paal, R., Reinhardt, B., Renné, D., Sengupta, M., Wald, L., and Wilbert, S.: Direct normal irradiance related definitions and applications: The circumsolar issue, Solar Energy, 110, 561–577, https://doi.org/10.1016/j.solener.2014.10.001, 2014.

Bolsée, D.: Métrologie de la spectrophotométrie solaire absolue. Principes, mise en oeuvre et résultats. Instrument SOLSPEC à bord de la Station Spatiale Internationale. Ph.D. thesis, Free University of Brussels, 2012.

Bolsée, D., Pereira, N., Decuyper, W., Gillotay, D., Yu, H., Sperfeld, P., Pape, S., Cuevas, E., Redondas, A., Hernandéz, Y., and Weber, M.: Accurate Determination of the TOA Solar Spectral NIR Irradiance Using a Primary Standard Source and the Bouguer–Langley Technique, Solar Physics, 289, 2433–2457, https://doi.org/10.1007/s11207-014-0474-1, http://dx.doi.org/10.1007/s11207-014-0474-1, 2014.

Bolsée, D., Pereira, N., Cuevas, E., García, R., and Redondas, A.: Comments to the Article by Thuillier et al. "The Infrared Solar Spectrum Measured by the SOLSPEC Spectrometer Onboard the International Space Station" on the Interpretation of Ground-based Measurements at the Izaña Site, Solar Physics, 291, 2473–2477, https://doi.org/10.1007/s11207-016-0914-1, 2016.

Elsey, J., Coleman, M. D., Gardiner, T., and Shine, K. P.: Can Measurements of the Near-Infrared Solar Spectral Irradiance be Reconciled? A New Ground-Based Assessment Between 4,000 and 10,000 cm-1, Geophysical Research Letters, 44, 10,071–10,080, https://doi.org/10.1002/2017gl073902, 2017.

Ermolli, I., Matthes, K., Dudok de Wit, T., Krivova, N. A., Tourpali, K., Weber, M., Unruh, Y. C., Gray, L., Langematz, U., Pilewskie, P., Rozanov, E., Schmutz, W., Shapiro, A., Solanki, S. K., and Woods, T. N.: Recent variability of the solar spectral irradiance and its impact on climate modelling, Atmospheric Chemistry and Physics, 13, 3945–3977, https://doi.org/10.5194/acp-13-3945-2013, https://www.atmos-chem-phys.net/13/3945/2013/, 2013.

Friedrich, R., Fischer, J., and Strock, M.: Accurate calibration of filter radiometers against a cryogenic radiometer using a trap detector, Metrologia, 32, 509–513, 1995.

Gray, L. J., Beer, J., Geller, M., Haigh, J. D., Lockwood, M., Matthes, K., Cubasch, U., Fleitmann, D., Harrison, G., Hood, L., Luterbacher, J., Meehl, G. A., Shindell, D., van Geel, B., and White, W.: SOLAR INFLUENCES ON CLIMATE, Reviews of Geophysics, 48, https://doi.org/10.1029/2009RG000282, https://agupubs.onlinelibrary.wiley.com/doi/abs/10.1029/2009RG000282, 2010.

Gröbner, J. and Kerr, J. B.: Ground-based determination of the spectral ultraviolet extraterrestrial solar irradiance: Providing a link between space-based and ground-based solar UV measurements, Journal of Geophysical Research: Atmospheres, 106, 7211–7217, https://doi.org/10.1029/2000JD900756, https://agupubs.onlinelibrary.wiley.com/doi/abs/10.1029/2000JD900756, 2001.

Gröbner, J., Kröger, I., Egli, L., Hülsen, G., Riechelmann, S., and Sperfeld, P.: The high-resolution extraterrestrial solar spectrum (QASUMEFTS) determined from ground-based solar irradiance measurements, Atmospheric Measurement Techniques, 10, 3375–3383, https://doi.org/10.5194/amt-10-3375-2017, https://www.atmos-meas-tech.net/10/3375/2017/, 2017.

Gueymard, C. A.: Parameterized transmittance model for direct beam and circumsolar spectral irradiance, Solar Energy, 71, 325–346, https://doi.org/10.1016/s0038-092x(01)00054-8, 2001.

Harder, J., Lawrence, G. M., Fontenla, J. M., Rottman, G., and Woods, T. N.: The Spectral Irradiance Monitor: Scientific requirements, instrument design, and operation modes, Solar Phys., 230, 141–167, 2005.

Harder, J., Lawrence, G., Rottman, G. J., and Woods, T. N.: The Spectral Irradiance Monitor (SIM) for the SORCE mission, In: Barnes, W.L. (ed.), *Earth Observing Systems V., Proc. SPIE*, 4135, 204–214, 2000a.

Harder, J. W., Fontenla, J. M., Pilewskie, P., Richard, E. C., and Woods, T. N.: Trends in solar spectral irradiance variability in the visible and infrared, Geophys. Res. Lett, 36, L07 801, 2009.

Harder, J. W., Thuillier, G., Richard, E. C., Brown, S. W., Lykke, K. R., Snow, M., McClintock, W. E., Fontenla, J. M., Woods, T. N., and Pilewskie, P.: The SORCE SIM solar spectrum: Comparison with recent observations, Solar Phys., 263, 3–24, 2010.

Hilbig, T., Weber, M., Bramstedt, K., Noel, S., Burrows, J. P., Krijge, J. M., Snel, R., Meftah, M., Dame, L., Bekki, S., Bolsee, D., Pereira, N., and Sluse, D.: The New SCIAMACHY Reference Solar Spectral Irradiance and its Validation, Solar Physics, submitted, 2018.

Kasten, F. and Young, A. T.: Revised optical air mass tables and approximation formula, Applied Optics, 28, 4735, https://doi.org/10.1364/ao.28.004735, 1989.

Kiedron, P. W. and Michalsky, J. J.: Non-parametric and least squares Langley plot methods, Atmospheric Measurement Techniques, 9, 215–225, https://doi.org/10.5194/amt-9-215-2016, 2016.

Kindel, B. C., Qu, Z., and Goetz, A. F. H.: Direct solar spectral irradiance and transmittance measurements from 350 to 2500 nm, Appl. Opt., 40, 3483–3494, 2001.

Krystek, M. and Anton, M.: A weighted total least-squares algortihm fot fitting a straight line, Meas. Sci. Technol., 18, 3438–3442, 2007.

Lean, J.: Variations in the Sun's radiative output, Reviews of Geophysics, 29, 505–535, https://doi.org/10.1029/91RG01895, https://agupubs.onlinelibrary.wiley.com/doi/abs/10.1029/91RG01895, 1991.

Mayer, B. and Kylling, A.: Technical note: The libRadtran software package for radiative transfer calculations - description and examples of use, Atmospheric Chemistry and Physics, 5, 1855–1877, https://doi.org/10.5194/acp-5-1855-2005, 2005.

Meeus, J.: Astronomical Algorithms, Willmann-Bell, https://www.amazon.com/Astronomical-Algorithms-Jean-Meeus/dp/0943396611?SubscriptionId=0JYN1NVW651KCA56C102&tag=techkie-20&linkCode=xm2&camp=2025&creative=165953&creativeASIN=0943396611, 1998.

Meftah, M., Damé, L., Bolsée, D., Pereira, N., Sluse, D., Cessateur, G., Irbah, A., Sarkissian, A., Djafer, D., Hauchecorne, A., and Bekki, S.: A New Solar Spectrum from 656 to 3088 nm, Solar Physics, 292, https://doi.org/10.1007/s11207-017-1115-2, 2017.

Menang, K. P., Ptashnik, I. V., Coleman, M., Gardiner, T., and Shine, K.: A high-resolution near-infrared extraterrestrial solar spectrum derived from ground-based Fourier transform spectrometer measurements, J. Geophys. Res., 118, 1–13, 2013.

Noël, S., Bovensmann, H., Burrows, J. P., Frerick, J., Chance, K. V., Goede, A. P., and Muller, C.: SCIAMACHY instrument on ENVISAT-1, In: Fujisada, H. (ed.), *Sensors, Systems, and Next-Generation Satellites II., Proc. SPIE*, 3498, 94–104, 1998.

Sapritsky, V. I., Khlevnoy, B. B., Khromchenko, V. B., Lisiansky, B. E., Mekhontsev, S. N., Melenevsky, U. A., Morozova, S. P., Prokhorov, A. V., Samoilov, L. N., Shapoval, V. I., Sudarev, K. A., and Zelener, M. F.: Precision blackbody sources for radiometric standards, Appl. Opt, 36, 5403–5408, 1997.

Schmid, B. and Wehrli, C.: Comparison of Sun photometer calibration by use of the Langley technique and the standard lamp, Appl. Opt., 34, 4500–4512, 1995.

Shaw, G. E.: Solar Spectral Irradiance: The Role of Earth-Based Measurements, in: The Solar Constant and the Earth's Atmosphere, Proceedings of the Workshop held at Big Bear Solar Observatory, Big Bear City, CA, 19-21 May 1975. Big Bear Solar Observatory, edited by by H. Zirin, E. and J. Walter, ., p. 210, 1975.

Shaw, G. E.: Error analysis of multi-wavelength sun photometry, pure and applied geophysics, 114, 1–14, https://doi.org/10.1007/BF00875487, https://doi.org/10.1007/BF00875487, 1976.

Shaw, G. E.: Solar spectral irradiance and atmospheric transmission at Mauna Loa Observatory, Applied Optics, 21, 2006, https://doi.org/10.1364/ao.21.002006, 1982.

Sperfeld, P., Metzdorf, J., Galal Yousef, S., Stock, K. D., and Müller, W.: Improvement and extension of the black-body-based spectral irradiance scale, Metrologia, 35, 267–271, 1998a.

Sperfeld, P., Galal Yousef, S., Metzdorf, J., N., B., and Müller, W.: The use of self-consistent calibrations to recover absorption bands in the black-body spectrum, Metrologia, 37, 373–376, 2000.

Taubert, D., Friedrich, R., Hartmann, J., and Hollandt, J.: Improved calibration of the spectral responsivity of Interference Filter Radiometers in the visible and near infrared spectral range at PTB, Metrologia, 40, S35–38, 2003.

Thuillier, G., Simon, P. C., Labs, D., Pastiels, R., and Neckel, H.: An instrument to measure the solar spectrum from 170 to 3200 nm on board Spacelab, Solar Phys., 74, 531–537, 1981.

Thuillier, G., Hersé, M., Labs, D., Foujols, T., Peetermans, W., Gillotay, D., Simon, P. C., and Mandel, H.: The solar spectral irradiance from 200 to 2400 nm as measured by the SOLSPEC spectrometer from the ATLAS and EURECA missions, Solar Phys., 214, 1–22, 2003.

Thuillier, G., Foujols, T., Bolsée, D., Gillotay, D., Hersé, M., Peetermans, W., Decuyper, W., Mandel, H., Sperfeld, P., Pape, S., Taubert, D. R., and Hartmann, J.: SOLAR/SOLSPEC: Scientific objectives, instrument performance and its absolute calibration using a blackbody as primary standard source, Solar Phys., 257, 185–213, 2009.

Thuillier, G., Bolsée, D., Schmidtke, G., Foujols, T., Nikutowski, B., Shapiro, A., Schmutz, W., Brunner, R., Erhardt, C., Hersé, M., Gillotay, D., Petermanns, W., Decuyper, W., Pereira, N., and Mandel, H.: The solar irradiance spectrum at solar activity minimum between solar cycles 23 and 24, Solar Phys., p. submitted, 2013.

Weber, M.: Comment on the Article by Thuillier et al. "The Infrared Solar Spectrum Measured by the SOLSPEC Spectrometer onboard the International Space Station", Solar Physics, 290, 1601–1605, https://doi.org/10.1007/s11207-015-0707-y, 2015.

Werner, L., Fischer, J., Johannsen, U., and Hartmann, J.: Accurate determination of the spectral responsivity of silicon trap detectors between 238 and 1015 nm,, Metrologia, 37, 279–284, 2000.

Appendix A: Appendix A

Atmos. Meas. Tech. Discuss., https://doi.org/10.5194/amt-2018-160
Manuscript under review for journal Atmos. Meas. Tech.
Discussion started: 3 July 2018

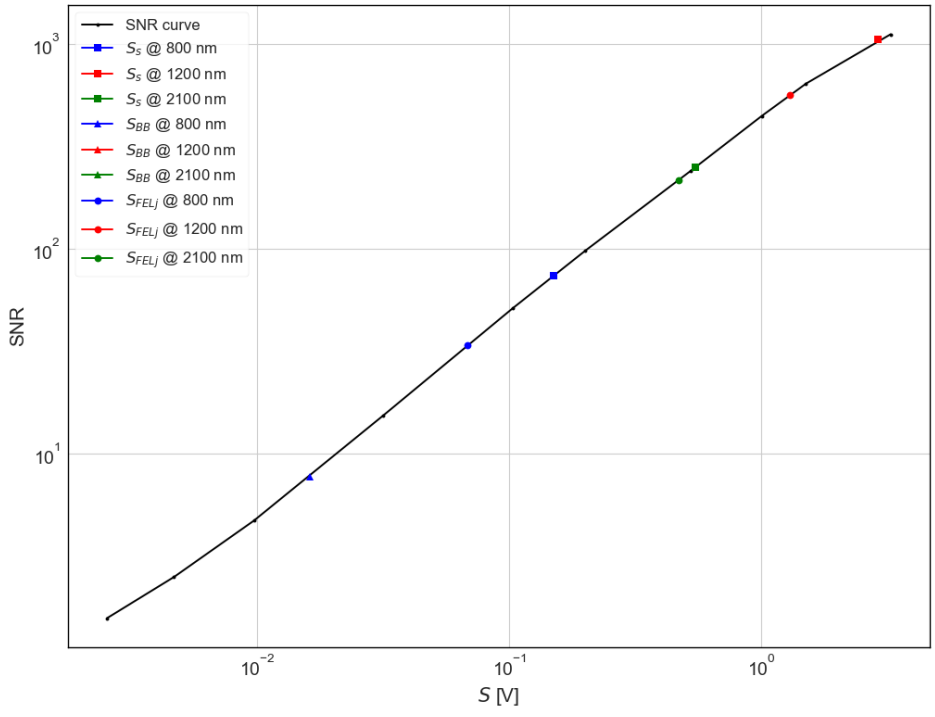

Figure A1. Spectrometer's SNR curve. SNR is defined as $\frac{<S>}{\sigma(S)}$. S is an accumulation of measurements in front of a stable lamp. For reference, the SNR values for Solar, blackbody and lamp signals at specific wavelengths is also shown.

Atmos. Meas. Tech. Discuss., https://doi.org/10.5194/amt-2018-160
Manuscript under review for journal Atmos. Meas. Tech.
Discussion started: 3 July 2018

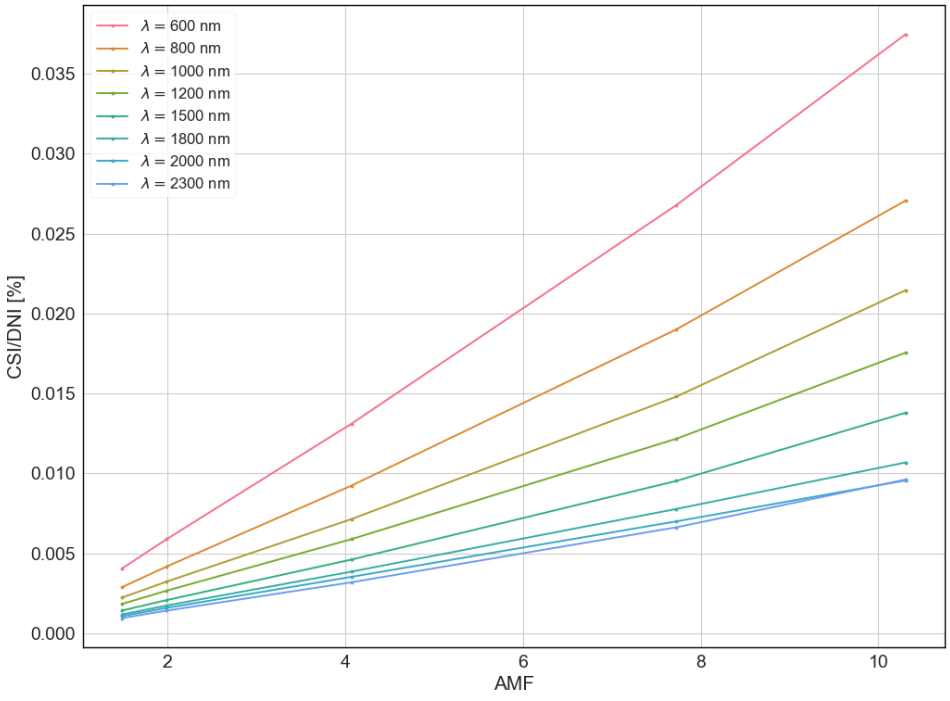

Figure A2. Modelled percentage of circumsolar irradiance relative to normal direct irradiance, entering the detector as a function of wavelength and AMF. Circumsolar irradiance has a negligible effect on the measured irradiance even for the highest circumsolar conditions (lower wavelengths and high AMF)

Atmos. Meas. Tech. Discuss., https://doi.org/10.5194/amt-2018-160
Manuscript under review for journal Atmos. Meas. Tech.
Discussion started: 3 July 2018

Atmospheric Measurement Techniques Discussions

Table A1. Aerosol Optical Depth (AOD) from AERONET data level 1.5. For each cell, the average AOD value and the variation in normalized standard deviation is shown.

Day of July 2016	870 nm	1020 nm	1640 nm
2AM	0.005 - 1.18%	0.007 - 4.6%	0.002 - 4.9%
3AM	0.005 - 2.0%	0.006 - 4.9%	0.002 - 3.8%
5AM	0.002 - 7.5%	0.007 - 2.7%	0.002 - 7.3%
9AM	0.006 - 2.0%	0.008 - 3.8%	0.002 - 5.6%
10AM	0.005 - 1.3%	0.008 - 3.2%	0.002 - 5.5%
11AM	0.005 - 1.7%	0.009 - 2.5%	0.002 - 3.7%
16AM	0.005 - 2.0%	0.008 - 5.7%	0.002 - 8.1%